C. R. Chimie 18 (2015) 1313–1319

Contents lists available at ScienceDirect

Comptes Rendus Chimie

www.sciencedirect.com

Full paper/Mémoire

A ruthenium(II) complex with the propionate ion: Synthesis, characterization and cytotoxic activity

Thalita M.P. Pagoto [a], Larissa L.G. Sobrinho [a], Angelica E. Graminha [b], Adriana P.M. Guedes [b], Murilo C. Carroccia [c], Pollyanna F. de Oliveira [d], Elisangela P. Silveira-Lacerda [e], Victor M. Deflon [c], Denise C. Tavares [d], Marcos Pivatto [a], Alzir A. Batista [b], Gustavo Von Poelhsitz [a,*]

[a] Instituto de Química, Universidade Federal de Uberlândia, CP 593, CEP 38400-902, Uberlândia (MG), Brazil
[b] Departamento de Química, Universidade Federal de São Carlos, CP 676, CEP 13565-905, São Carlos (SP), Brazil
[c] Instituto de Química de São Carlos, Universidade de São Paulo, CP 780, CEP 13566-590, São Carlos (SP), Brazil
[d] Universidade de Franca, CEP 14404-600, Franca(SP), Brazil
[e] Instituto de Ciências Biológicas, Universidade Federal de Goiás, CP 2425-0, CEP 74690-970, Goiânia (GO), Brazil

ARTICLE INFO

Article history:
Received 13 May 2015
Accepted after revision 8 July 2015
Available online 28 August 2015

Keywords:
Ruthenium
Biological activity
Mass spectrometry
Carboxylate ligands
Phosphane ligands
X-Ray diffraction

ABSTRACT

The complex $[Ru(\eta^2\text{-}O_2CCH_2CH_3)(dppe)_2]PF_6$ (dppe = 1,2-bis(diphenylphosphino)ethane) was prepared and characterized by elemental analysis, spectroscopic techniques, X-ray crystallography, HRESIMS and HRESIMS/MS. The characterization data are consistent with a *cis* arrangement for the dppe ligands and a bidentate coordination of the propionate ligand through carboxylate oxygens. Cytotoxicity assays were carried out on human and murine cancer and normal cell lines. In general, the $[Ru(\eta^2\text{-}O_2CCH_2CH_3)(dppe)_2]PF_6$ complex was more cytotoxic than both its precursor *cis*–$[RuCl_2(dppe)_2]$ and the reference metallodrug cisplatin. The best results against the HepG2 human tumour cell line and S180 murine tumour cell line were found with IC_{50} values of 6.5 ± 0.2 and 0.18 ± 0.03 μM, respectively.

1. Introduction

It is well established that metal-based chemotherapy is an option for cancer treatment [1–5]. The success of cisplatin, carboplatin and oxaliplatin against ovarian, bladder and testicular cancers has stimulated the search for cytotoxic non-platinum metal compounds with more acceptable toxicity profiles and expanded activities [1,6–8]. Some of these non-platinum compounds have shown promising activity, with biological features including mechanism of action, toxicity and biodistribution, which are very different from those of classical platinum compounds and might therefore be active against resistant human cancers [9–12].

Ruthenium compounds are a promising alternative to platinum and, among them, NAMI-A–[ImH][*trans*-$RuCl_4$(DMSO)(Im)] and KP1019–[ImH][*trans*-$RuCl_4(Im)_2$] (Im = imidazole) have favourable *in vitro* and *in vivo* pharmacological properties and are currently in clinical trials [13–18]. Distinct from platinum drugs, these ruthenium complexes act on metastatic tumours. Also, ruthenium compounds can be useful in the treatment of platinum-drug-resistant tumours [16,19].

Previous work from our group displayed biological results from the diphosphinic ruthenium(II) precursor *cis*–$[RuCl_2(P\text{–}P)_2]$, P–P = dppm or dppe, and derivatives with a

* Corresponding author.
E-mail address: gustavo@iqufu.ufu.br (G. Von Poelhsitz).

http://dx.doi.org/10.1016/j.crci.2015.07.008
1631-0748/

2-pyridinecarboxylic acid anion (pic) of the type *cis*–[Ru(pic)(P–P)$_2$]PF$_6$ [20,21]. The antimycobacterial activity against MTB H$_{37}$Rv indicated a MIC close to 25 μM for the precursor and a much higher activity for the *cis*–[Ru(pic)(P–P)$_2$]PF$_6$, with a minimum inhibitory concentration (MIC) in the low micromolar range (0.22 to 0.69 μM) [20]. Additional studies performed with the *cis*–[Ru(pic)(dppe)$_2$]PF$_6$ complex revealed that the MIC value was maintained under various conditions, including acid pH, medium with 4% BSA and 10% FBS, and especially against variant strains resistant to tuberculosis reference drugs [21]. Its spectra of activity against *Staphylococcus aureus, Candida albicans* and *Mycobacterium smegmatis* were also evaluated and this ruthenium(II) complex showed MIC ranging from 0.3 to 5.3 μM [21]. An assay of acute oral toxicity for the *cis*-[Ru(pic)(dppe)$_2$]PF$_6$ indicated a class 5 compound (a substance with LD$_{50}$ greater than 2000 and less than 5000 mg/kg body weight), denoting a relatively low acute toxicity [21].

Due to this background of promising biological results focusing mainly on a single derivative of *cis*–[RuCl$_2$(dppe)$_2$], our current strategy consists in evaluating other derivatives with different chelating moieties replacing the chlorido ligands in the search for new cytotoxic agents against tumour cells. The propionate ion was introduced in the coordination sphere of the complex with the aim of obtaining a compound with good solubility in the culture medium. In this work, the synthesis and characterization, including X-ray structure, of the complex [Ru(η^2-O$_2$CCH$_2$CH$_3$)(dppe)$_2$]PF$_6$ are reported. In addition, preliminary *in vitro* tests of cytotoxic activities against a variety of human and murine cell lines are presented and discussed.

2. Experimental

2.1. General

Solvents were purified by standard methods. All chemicals used were of reagent grade or comparable purity. The RuCl$_3$·3H$_2$O and the ligands 1,2-*bis*(diphenylphosphino)ethane (dppe) and sodium propionate (NaO$_2$CCH$_2$CH$_3$) were used as received from Aldrich. The *cis*–[RuCl$_2$(dppe)$_2$] precursor complex was prepared according to a literature method [22].

2.2. Instrumentation

IR spectra were recorded on a Shimadzu FTIR-Prestige 21 spectrophotometer using KBr pellets. UV–Vis spectroscopy was performed on a Femto model 800 XI spectrophotometer using cuvettes with a 1-cm path length. ^{31}P{^{1}H} NMR was performed at 293 K on a Bruker DRX 400 MHz spectrometer with a BBO 5-mm probe at 298 K. The NMR spectra were recorded in CDCl$_3$ with 85% H$_3$PO$_4$ as an external reference. A high-resolution mass spectrum (HRESIMS) with electrospray ionization was measured on an ultrOTOF (Bruker Daltonics) spectrometer, operating in the positive mode. Methanol was used as the solvent and the sample was infused into the ESI source at a flow rate of 5 μL/min. The calculated values for the charged complex ion were made using ChemDraw Ultra 12.0. Elemental analyses were performed on a PerkinElmer 2400 Series II CHNS/O microanalyser.

2.3. Synthesis of *[Ru(η^2-O$_2$CCH$_2$CH$_3$)(dppe)$_2$]PF$_6$*

The title complex was prepared by reacting the precursor *cis*–[RuCl$_2$(dppe)$_2$] (0.103 mmol; 100 mg) with an excess of sodium propionate (0.300 mmol; 28.8 mg) and 0.150 mmol (24.4 mg) of NH$_4$PF$_6$ in methanol (20 mL) at room temperature for 24 h. The final yellow solution was concentrated to ca. 3 mL and water was added for the precipitation of a pale yellow solid. The solid was filtered off, washed with water (3 × 5 mL) and diethyl ether (3 × 5 mL) and dried under reduce pressure.

Yield: 97.9 mg (85%). Anal. Calcd for C$_{55}$H$_{53}$F$_6$O$_2$P$_5$Ru: exptl (calc) C, 58.85 (59.20); H, 4.80 (4.79). ^{31}P{^{1}H} NMR (161.73 MHz): δ(ppm) 57.4 (triplet, 2P, $^2J_{P-P}$ = 18 Hz); 58.6 (triplet, 2P, $^2J_{P-P}$ = 18 Hz);−144.7 (septet, 1P, $^1J_{P-F}$ = 711 Hz). HRESIMS (MeOH): *m/z* 971.2051 [M–PF$_6$]$^+$ (calcd for [C$_{55}$H$_{53}$O$_2$P$_4$Ru], 971.2034). UV–Vis (CH$_2$Cl$_2$, 2.30 × 10^{-5} M): λ/nm (ε/M^{-1} cm^{-1}) 255 (5.29 × 10^4), 349 (2.16 × 10^3).

2.4. X-ray crystallography

Yellow crystals of the new ruthenium(II) complex were grown by slow evaporation of a dichloromethane solution at room temperature. The data collection was performed using Mo Kα radiation (λ = 0.71073 Å) on a BRUKER APEX II Duo diffractometer. Standard procedures were applied for data reduction and absorption correction. The structure was solved with SHELXS97 using direct methods [23] and all non-hydrogen atoms were refined with anisotropic displacement parameters with SHELXL97 [24]. The hydrogen atoms were calculated at idealized positions using the riding model option of SHELXL97 [24]. Table 1 presents more detailed information about the structural determination. The ORTEP view shown in Fig. 1 was prepared using ORTEP-3 for Windows.

2.5. Murine cell lines and culture conditions

Murine sarcoma-180 tumour cells (S-180) (ATCC®# TIB-66) and normal murine fibroblast cells (L-929) (ATCC®# CCL-1™) were cultured in suspension in RPMI 1640 and DMEM media (Sigma Chemical Co., MO), respectively, supplemented with 10% foetal calf serum, 100 μg/mL penicillin, and 100 μg/mL streptomycin. The cultures were incubated in a humidified incubator (Thermo Scientific) at 37 °C with 5% CO$_2$ according to previously described methods [25].

2.6. Cell viability assay related to murine cell lines

The cytotoxic effects were evaluated using an MTT assay with S-180 tumour cells and L-929 normal cells as described previously [26]. Briefly, 1.0 × 10^5 S-180 cells and 2.0 × 10^4 L-929 cells were plated in 96-well tissue culture plates and treated with different concentrations of ruthenium complex (0.2–200 μM) for 48 h. After treatment, 10 μL of MTT (5 mg mL^{-1}) were added to each well

Table 1
Crystallographic data and structural refinement details for $[Ru(\eta^2\text{-}O_2CCH_2CH_3)(dppe)_2]PF_6$.

Empirical formula	$C_{55}H_{53}O_2P_5F_6Ru$
M/g mol^{-1}	1115.89
Temperature/K	296(2)
Crystal system	Orthorhombic
Space group	*Pbca*
Unit cell dimensions	
a (Å)	16.0244(3)
b (Å)	21.9042(5)
c (Å)	29.5069(6)
V (Å^3)	10,357.0(4)
Z	8
Density (calc) (g·cm^{-3})	1.431
F(000)	4576
Crystal size (mm^3)	0.46 × 0.42 × 0.20
θ range data collection (°)	1.72–25.41
Index ranges	$-16 \le h \le 19$; $-26 \le k \le 23$; $-35 \le l \le 22$
Reflections collected	35,066
Independent reflections	9429
R_1	0.0318
wR_2	0.0746
Goodness-of-fit on F^2	1.037

and the plates were incubated at 37 °C for an additional 3 h. The purple formazan crystals were dissolved in 50 μL of SDS, and the absorbance was determined at 545 nm using a Stat Fax 2100 microplate reader (Awareness Technology, Palm City, FL, USA). The cell viability was calculated as follows: viability (%) = (absorbance of the treated wells)/(absorbance of the control wells) × 100. The IC_{50} (complex concentration (μM) that results in a 50% reduction in cellular viability) was obtained by plotting % cell viability versus drug concentration using GraphPad Prism 4.02 for Windows (GraphPad Software, San Diego, CA, USA).

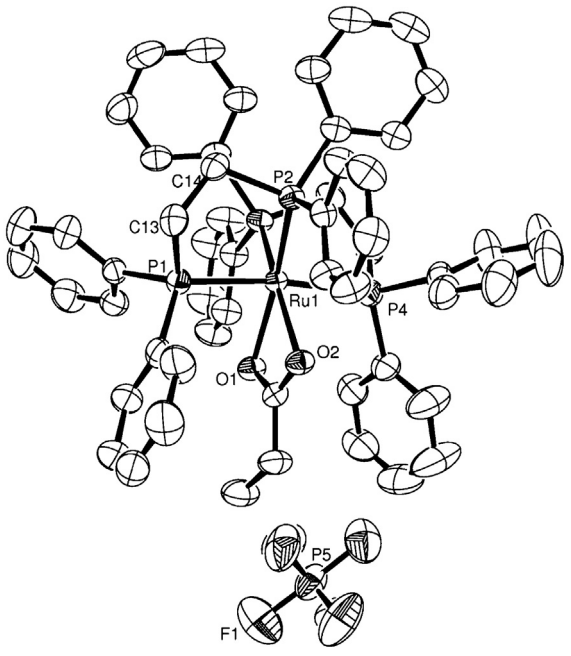

Fig. 1. ORTEP view of the $[Ru(\eta^2\text{-}O_2CCH_2CH_3)(dppe)_2]PF_6$ complex showing the atom labelling and the 50% probability ellipsoids.

2.7. Human cell lines and culture conditions

For the experiments, four different human cell lines from the 4th through the 12th passages were used: HepG2 (hepatocellular carcinoma), MCF-7 (breast adenocarcinoma), MO59 J (glioblastoma) and GM07492A (normal lung fibroblasts). The different cell lines were maintained as monolayers in plastic culture flasks (25 cm^2) containing HAM-F10 plus DMEM (1:1; Sigma-Aldrich) or only DMEM, depending on the cell line, supplemented with 10% foetal bovine serum (Nutricell) and 2.38 mg/mL Hepes (Sigma-Aldrich) at 37 °C in a humidified 5% CO_2 atmosphere. Antibiotics (0.01 mg/mL streptomycin and 0.005 mg/mL penicillin; Sigma-Aldrich) were added to the medium to prevent bacterial growth.

2.8. Cell viability assay related to human cell lines

Cytotoxic activity on the cell lines was assessed using the Colorimetric Assay *In Vitro* Toxicology–XTT Kit (Roche Diagnostics). For the experiments, 1×10^4 cells were seeded into microplates with 100 μL of culture medium (1:1 HAM F10 + DMEM or DMEM alone) supplemented with 10% foetal bovine serum containing concentrations of essential oils ranging from 1.565 to 1600 μg/mL. Negative (no treatment), solvent (0.02% DMSO) and positive (25% DMSO) controls were included. Positive controls comprising doxorubicin (DXR, Pharmacia Brasil Ltda., 98% purity), (*S*)-(+)-camptothecin (CPT, Sigma-Aldrich, ≥ 90% purity), etoposide (VP16, Sigma-Aldrich, ≥ 98% purity) and cisplatin (Sigma-Aldrich, ≥ 98% purity) were included. After incubation at 36.5 °C for 24 h, the culture medium was removed and cells were washed with 100 μL of PBS to remove the treatments, after which they were exposed to 100 μL of HAM-F10 culture medium without phenol red. Then, 25 μl of XTT were added and the cells were incubated at 36.5 °C for 17 h. The absorbance of the samples was determined using a multi-plate reader (ELISA–Tecan–SW Magellan vs 5.03 STD 2P) at a wavelength of 450 nm and a reference length of 620 nm.

2.9. Statistical analysis related to human cell line assays

Cytotoxicity was assessed using the IC_{50} response parameter (50% cell growth inhibition) calculated with the GraphPad Prism program, plotting cell survival against the respective concentrations of the treatments. One-way ANOVA was used for the comparison of means ($P < 0.05$). The selectivity index was calculated by dividing the IC_{50} value of the isolated compounds on GM07492-A cells by the IC_{50} value determined for human cancer cells.

3. Results and discussion

3.1. Synthesis

The simple reaction of sodium propionate with the ruthenium(II) diphosphine precursor complex *cis*–$[RuCl_2(dppe)_2]$ resulted in the product $[Ru(\eta^2\text{-}O_2CCH_2CH_3)(dppe)_2]PF_6$, by simple chlorido exchange under mild conditions (see Scheme 1).

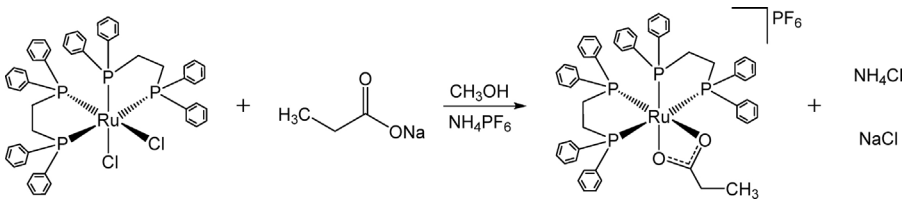

Scheme 1. Route for the synthesis of $[Ru(\eta^2\text{-}O_2CCH_2CH_3)(dppe)_2]PF_6$.

The similar compound $[Ru(\eta^2\text{-}O_2CCH_2CH_3)(dppe)_2]BPh_4$ was previously described, prepared via a different method than the one presented here, by reacting the ruthenium(II, III) propionate precursor with dppe [27].

3.2. Structural studies

The X-ray structure of $[Ru(\eta^2\text{-}O_2CCH_2CH_3)(dppe)_2]PF_6$ was determined and the ORTEP drawing showing the atom numbering scheme is depicted in Fig. 1. Relevant bond lengths and angles for the cationic complex cation are presented in Table 2.

The $[Ru(\eta^2\text{-}O_2CCH_2CH_3)(dppe)_2]^+$ complex adopts a distorted octahedral geometry for the ruthenium centre, which is coordinated by two *cis* positioned dppe ligands and with the propionate ligand completing the coordination sphere. Distortions are caused by the chelate bite angles of 82.91(2) and 83.46(2)° imposed by the ethylene bridge of the dppe ligands and by the carboxylate group of the propionate ligand, resulting in the O(1)–Ru–O(2) angle of only 59.44(6)°. Such a small bite angle for the propionate ligand is quite similar to that observed for the related acetate ligand [27,28]. The Ru–P bond lengths vary from 2.3679(6) to 2.3809(7) Å for mutually *trans* disposed phosphorus atoms and from 2.2946(7) to 2.3166(6) Å for phosphorus atoms *trans* positioned to propionate oxygen atoms. These marked differences clearly illustrate the greater *trans*-influence of phosphorus when compared with oxygen [29–31]. The propionate ligand is coordinated in an almost symmetrical manner as illustrated by the Ru–O distances of 2.1787(16) and 2.1983 (17) Å. These values are in the range reported for similar compounds [28,32,33].

3.3. Spectroscopic characterization

The $^{31}P\{^1H\}$ NMR spectrum of $[Ru(\eta^2\text{-}O_2CCH_2CH_3)(dppe)_2]PF_6$ showed a pair of triplet resonance signals centred at 57.4 and 58.6 ppm, with the splitting pattern closer to an A_2B_2 pattern ($\Delta\nu/J = 11.1$). These signals are very similar to that found for the $[Ru(\eta^2\text{-}O_2CCH_3)(dppe)_2]PF_6$ analogous (triplets at 57.02 and 55.32 ppm) previously published [32] and downfield shifted when compared with the triplet signals for the *cis*–$[RuCl_2(dppe)_2]$ that are observed at 37.4 and 50.3 ppm with $^2J_{P-P} = 19.5$ Hz [22].

The IR spectrum displayed the typical asymmetric (ν_{asym}) and symmetric (ν_{sym}) carboxylate stretching frequencies at 1500 and 1452 cm^{-1} ($\Delta = 48$ cm^{-1}), respectively, confirming the presence of the propionate ligand coordinated in the chelating mode to the metal centre [34]. In the free ligand $NaO_2CCH_2CH_3$, the $\nu_{as}COO^-$and ν_sCOO^-vibrational modes appeared at 1662 and 1429 cm^{-1} [35].

Table 2
Selected bond distances (Å) and angles (°) for the $[Ru(\eta^2\text{-}O_2CCH_2CH_3)(dppe)_2]PF_6$ complex.

Ru(1)–O(1)	2.1787(16)	O(1)–Ru(1)–O(2)	59.44(6)
Ru(1)–O(2)	2.1983(17)	P(2)–Ru(1)–P(1)	82.91(2)
Ru(1)–P(3)	2.2946(7)	P(3)–Ru(1)–P(4)	83.46(2)
Ru(1)–P(2)	2.3166(6)	O(1)–Ru(1)–P(2)	161.29(5)
Ru(1)–P(1)	2.3679(6)	O(2)–Ru(1)–P(3)	160.92(5)
Ru(1)–P(4)	2.3809(7)	P(1)–Ru(1)–P(4)	173.18(2)
O(2)–C(53)	1.267(3)	C(53)–O(2)–Ru(1)	90.88(14)
O(1)–C(53)	1.266(3)	C(53)–O(1)–Ru(1)	91.81(14)
C(53)–C(54)	1.500(4)	O(1)–C(53)–C(54)	121.8(2)
C(54)–C(55)	1.504(4)	O(2)–C(53)–C(54)	120.3(2)

3.4. HRESI mass spectrometry

The mass spectra of complexes containing ruthenium are characterised by their isotopic pattern demonstrated by the presence of ^{96}Ru (5.5%), ^{98}Ru (1.9%), ^{99}Ru (12.7%), ^{100}Ru (12.6%), ^{101}Ru (17.1%), ^{102}Ru (31.6%) and ^{104}Ru (18.6%) isotopes, with the nuclide abundance in parentheses. A high-resolution mass spectrum of the $[Ru(\eta^2\text{-}O_2CCH_2CH_3)(dppe)_2]PF_6$ was recorded and the data confirmed the established pattern (Fig. 2a). In this study, the *m/z* values listed below in the text refer to the peak of the most abundant element corresponding to the ^{102}Ru isotope. The ion complex was observed at *m/z* 971.2051 $[M]^+$, in agreement with the calculated value for $C_{55}H_{53}O_2P_4Ru$, 971.2034. Collision-induced dissociation (CID) experiments (MS/MS) with an increasing collisional energy using N_2 as the collision gas under the selected ion at *m/z* 971.2051 showed a fragmentation pathway with an initial loss of 74 *u* proposed for a neutral elimination of propionic acid (Figs. 2b and 3). Two additional neutral eliminations were observed at *m/z* 685 and 499, and were attributed to the decomplexation of portions of the ligands as a diphenyl(vinyl)phosphine (212 *u*) and a diphenylphosphine (186 *u*), respectively (Figs. 2b and 3).

3.5. Cytotoxicity assays

Human and murine cell lines were exposed to the ruthenium(II) complexes and cisplatin for periods of 24 and 48 h, respectively, in order to allow them to reach DNA or any other biological target. The IC_{50} values calculated from the dose–survival curves generated by the XTT or MTT assays obtained after drug treatment are shown in Table 3.

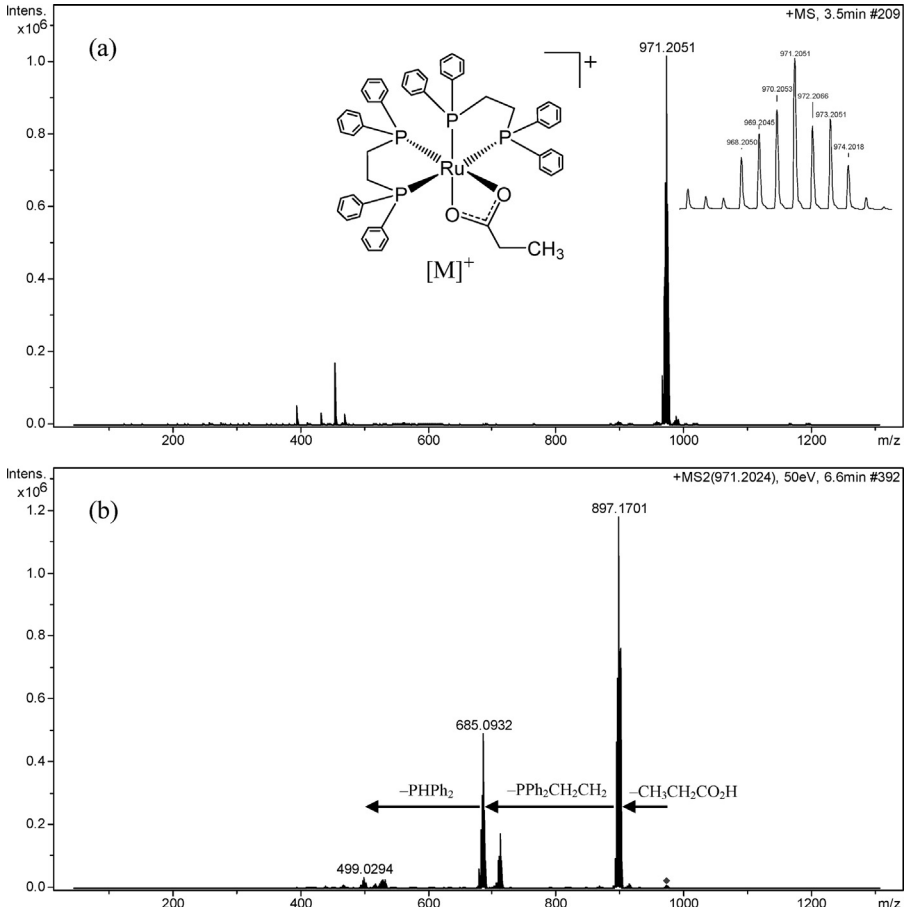

Fig. 2. ESI mass spectra of $[Ru(\eta^2\text{-}O_2CCH_2CH_3)(dppe)_2]^+$. (a) HRESI–MS spectrum of $[Ru(\eta^2\text{-}O_2CCH_2CH_3)(dppe)_2]^+$ *m/z* 971.2051 $[M]^+$ (calcd for $C_{55}H_{53}O_2P_4Ru$, 971.2034) and (b) ESI–MS/MS spectrum of *m/z* 971.2051.

The $[Ru(\eta^2\text{-}O_2CCH_2CH_3)(dppe)_2]PF_6$ complex showed high cytotoxicity against all the human tumour cell lines assayed, with IC_{50} values close to 7 μM. The best result was obtained against the human hepatocellular carcinoma HepG2 cell line with an IC_{50} of 6.5 ± 0.2 μM, this value being practically identical to that found for the reference metallodrug cisplatin. Against the normal cell line GM07492A, a 3-fold smaller cytotoxic effect of cisplatin was observed when compared with $[Ru(\eta^2\text{-}O_2CCH_2CH_3)(dppe)_2]PF_6$. The selectivity index–SI (SI = IC_{50} GM07492A/IC_{50} human tumour cell line) was very close to 1 for all the cell lines assayed, indicating a lack of selectivity of the complex. Under the same experimental conditions, the precursor complex *cis*–$[RuCl_2(dppe)_2]$ was much less active than the propionate derivative by factors ranging from 14 to 38. A similar increase in activity was also observed against the normal cell line GM07492A. The lack of selectivity was also observed for *cis*–$[RuCl_2(dppe)_2]$, with SI values close to 1 or less. These data clearly indicate that exchanging two chlorido ligands for a bidentate carboxylate group renders the complex very cytotoxic, probably due its greater solubility and availability in the culture medium.

The $[Ru(\eta^2\text{-}O_2CCH_2CH_3)(dppe)_2]PF_6$ complex showed significant cytotoxicity against S180 murine sarcoma cells,

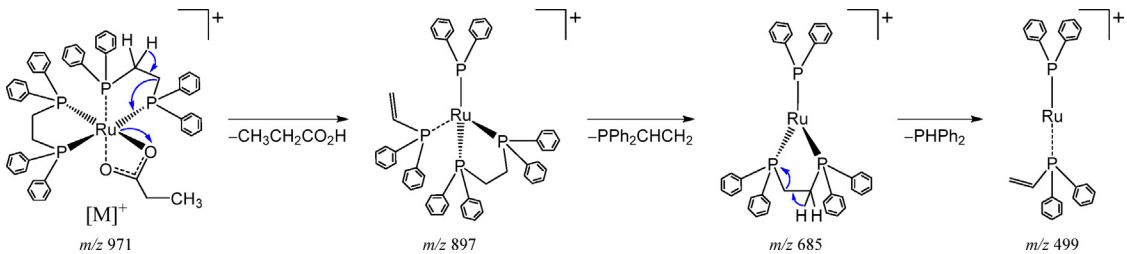

Fig. 3. Fragmentation pathway proposed for $[Ru(\eta^2\text{-}O_2CCH_2CH_3)(dppe)_2]^+$.

Table 3
Inhibitory activities of ruthenium complexes and cisplatin against normal and tumour cell lines, expressed as IC_{50} ($\mu mol\,L^{-1}$).

Compound	Cell line					
	GM07492A*	HepG2*	MCF-7*	MO59 J*	S180#	L929#
cis–[$RuCl_2(dppe)_2$]	107 ± 28	102 ± 19	269 ± 10	98 ± 7	n.d.	n.d.
[$Ru(\eta^2\text{-}O_2CCH_2CH_3)(dppe)_2$]$PF_6$	8.0 ± 0.4	6.5 ± 0.2	7.0 ± 0.4	7 ± 2	0.18 ± 0.03	1.3 ± 0.5
cisplatin	26 ± 3	6.3 ± 0.7	34 ± 4	22 ± 4	64.8 ± 0.2	29 ± 2

GM07492A (normal human lung fibroblasts), HepG2 (human hepatocellular carcinoma), MCF-7 (human breast adenocarcinoma), MO59 J (human glioblastoma), S180 (murine sarcoma), L929 (normal murine fibroblasts). *24 h incubation; #48 h incubation

with IC_{50} in the low micromolar range ($IC_{50} = 0.18 \pm 0.03\ \mu M$). In L929 normal murine fibroblast cell line, this complex was still very active with an IC_{50} value of $1.3 \pm 0.5\ \mu M$, resulting in a SI of 7 (SI = IC_{50} L929/IC_{50} S180). Under the same experimental conditions the metal-based reference cytotoxic drug cisplatin showed moderate to low activity, with an IC_{50} value of $64.8 \pm 0.2\ \mu M$ in the tumour cells, meaning that the compound was 360-fold less active than the ruthenium complex. Also, cisplatin showed greater active against normal cells than tumour cells, resulting in a SI of 0.45.

Data displayed in Table 3 indicate that the new ruthenium complex has some characteristics that increased its activity against murine cells when compared with human cells. Interestingly, cisplatin does not share this behaviour and was less cytotoxic against the murine cells.

These data suggest that ruthenium(II) containing diphosphines and carboxylates are potential cytotoxic agents and should be studied further.

4. Conclusion

In this investigation a ruthenium(II) complex containing dppe and the propionate anion with formula [$Ru(\eta^2\text{-}O_2CCH_2CH_3)(dppe)_2$]$PF_6$ was synthesized and characterized by elemental analysis, spectroscopic methods, X-ray diffraction, HRESIMS and HRESIMS/MS. The spectroscopic analyses were in agreement with the structure found by X-ray diffraction, with the propionate chelated by the carboxylate group. The *in vitro* cytotoxicity activity assays of the ruthenium complex indicated high cytotoxicity against human tumour cell lines and very high cytotoxicity against a murine sarcoma cell line; however, this complex lacks selectivity, as can be seen by its high cytotoxicity against normal cell lines. Interestingly, exchanging chlorido ligands for propionate resulted in higher activity, probably due its higher solubility and availability in the culture medium when compared with the precursor complex. Further studies are necessary to define the optimal biological targets for this kind of complex.

Acknowledgements

We thank CNPq, CAPES, FAPESP (Grant 2009/54011-8), the Minas Chemical Network (RQ-MG) and FAPEMIG (Grant APQ-04010-10).

Appendix A. Supplementary data

Coordinates and other crystallographic data have been deposited with the CCDC, deposition code CCDC 1033074. Copies of this information may be obtained from The Director, CCDC, 12 Union Road, Cambridge, CB2 1EZ, UK, Fax: +44 1233 336033, E mail: deposit@ccdc.cam.ac.uk or www.ccdc.cam.ac.uk.

References

[1] E. Wong, C.M. Giandomenico, Chem. Rev. 99 (1999) 2451–2466.
[2] M. Hartmann, B.K. Keppler, Comment. Inorg. Chem. 16 (1995) 339–372.
[3] L. Ronconi, P.J. Sadler, Coord. Chem. Rev. 251 (2007) 1633–1648.
[4] M.A. Jakupec, M. Galanski, V.B. Arion, C.G. Hartinger, B.K. Keppler, Dalton Trans. (2008) 183–194.
[5] K.D. Mjos, C. Orvig, Chem. Rev. 114 (2014) 4540–4563.
[6] M.J. Clarke, F.C. Zhu, D.R. Frasca, Chem. Rev. 99 (1999) 2511–2533.
[7] A.C. Komor, J.K. Barton, Chem. Commun. 49 (2013) 3617–3630.
[8] G. Colotti, A. Ilari, A. Boffi, V. Morea, Mini Rev. Med. Chem. 13 (2013) 211–221.
[9] I. Kostova, Curr. Med. Chem. 13 (2006) 1085–1107.
[10] W.H. Ang, P.J. Dyson, Eur. J. Inorg. Chem. (2006) 4003–4018.
[11] F. Guidi, A. Modesti, I. Landini, S. Nobili, E. Mini, L. Bini, M. Puglia, A. Casini, P.J. Dyson, C. Gabbiani, L. Messori, J. Inorg. Biochem. 118 (2013) 94–99.
[12] N. Muhammad, Z.J. Guo, Curr. Opin. Chem. Biol. 19 (2014) 144–153.
[13] B.K. Keppler, M.R. Berger, M.E. Heim, Cancer Treat. Rev. 17 (1990) 261–277.
[14] E. Alessio, G. Mestroni, A. Bergamo, G. Sava, Curr. Top. Med. Chem. 4 (2004) 1525–1535.
[15] M.A. Jakupec, V.B. Arion, S. Kapitza, E. Reisner, A. Eichinger, M. Pongratz, B. Marian, N.G.v. Keyserlingk, B.K. Keppler, Int. J. Clin. Pharm. Ther. 43 (2005) 595–596.
[16] C.G. Hartinger, S. Zorbas-Seifried, M.A. Jakupec, B. Kynast, H. Zorbas, B.K. Keppler, J. Inorg. Biochem. 100 (2006) 891–904.
[17] G. Sava, A. Bergamo, in: A. Bonetti, R. Leone, F.M. Muggia, S.B. Howell (Eds.), Ruthenium drugs for cancer chemotherapy: an ongoing challenge to treat solid tumours, in Platinum and Other Heavy Metal Compounds in Cancer Chemotherapy, Humana Press, New York, 2009
[18] P. Heffeter, A. Riabtseva, Y. Senkiv, C.R. Kowol, W. Koerner, U. Jungwith, N. Mitina, B.K. Keppler, T. Konstantinova, I. Yanchuk, R. Stoika, A. Zaichenko, W. Berger, J. Biomed. Nanotechnol. 10 (2014) 877–884.
[19] A. Bergamo, G. Sava, Dalton Trans. 40 (2011) 7817–7823.
[20] F.R. Pavan, G. Von Poelhsitz, F.B. do Nascimento, S.R.A. Leite, A.A. Batista, V.M. Deflon, D.N. Sato, S.G. Franzblau, C.Q.F. Leite, Eur. J. Med. Chem. 45 (2010) 598–601.
[21] F.R. Pavan, G. Von Poelhsitz, L.V.P. da Cunha, M.I.F. Barbosa, S.R.A. Leite, A.A. Batista, S.H. Cho, S.G. Franzblau, M.S. de Camargo, F.A. Resende, E.A. Varanda, C.Q.F. Leite, Plos One 8 (2013).
[22] M.T. Bautista, E.P. Cappellani, S.D. Drouin, R.H. Morris, C.T. Schweitzer, A. Sella, J. Zubkowski, J. Am. Chem. Soc. 113 (1991) 4876–4887.
[23] G.M. Sheldrick, Shelxs-97, Program for Crystal Structure Resolution, University of Göttingen, Göttingen, Germany, 1997.
[24] G.M. Sheldrick, Shelxs-97, Program for Crystal Structures Analysis, University of Göttingen, Göttingen, Germany, 1997.
[25] A.P. de Lima, F.d.C. Pereira, C.A. Sam Tiago Vilanova-Costa, A.d.S. Braga Barbosa Ribeiro, L.A. Pavanin, W.B. Dos Santos, E.d.P. Silveira-Lacerda, J. Biosciences 35 (2010) 371–378.
[26] T. Mosmann, J. Immunol. Methods 65 (1983) 55–63.

[27] E.B. Boyar, P.A. Harding, S.D. Robinson, C.P. Brock, J. Chem. Soc. Dalton Trans. (1986) 1771–1778.
[28] G.C. Jia, A.L. Rheingold, B.S. Haggerty, D.W. Meek, Inorg. Chem. 31 (1992) 900–904.
[29] N.T. Lucas, C.E. Powell, M.G. Humphrey, Acta Crystallogr. C 56 (2000) E392–E393.
[30] A.H. Murray, Z. Yue, A.I. Wallbank, T.S. Cameron, R. Vadavi, B.J. MacLean, M.A.S. Aquino, Polyhedron 27 (2008) 1270–1279.
[31] B.J. Coe, S.J. Glenwright, Coord. Chem. Rev. 203 (2000) 5–80.
[32] I.W. Wyman, T.J. Burchell, K.N. Robertson, T.S. Cameron, M.A.S. Aquino, Organometallics 23 (2004) 5353–5364.
[33] R.A. Sanchezdelgado, U. Thewalt, N. Valencia, A. Andriollo, R.L. Marquezsilva, J. Puga, H. Schollhorn, H.P. Klein, B. Fontal, Inorg. Chem. 25 (1986) 1097–1106.
[34] K. Nakamoto, Infrared and Raman Specta of Inorganic and Coordination Compounds, Part B, John Wiley and Sons, New York, 1997.
[35] R.I. Bickley, H.G.M. Edwards, R. Gustar, S.J. Rose, J. Mol. Struct. 248 (1991) 237–250.